OPEN ACCESS

Critical Current Density Measurements of Argyrodite Li_6PS_5Cl Solid Electrolyte at Ambient Pressure

Journal of The Electrochemical Society, 2023 **170** 100525

Critical Current Density Measurements of Argyrodite Li_6PS_5Cl Solid Electrolyte at Ambient Pressure

Artur Tron,[1] Ander Orue,[2] Pedro López-Aranguren,[2] and Alexander Beutl[1,z]

[1]*AIT Austrian Institute of Technology GmbH, Center for Low-Emission Transport, Battery Technologies, 1210 Vienna, Austria*
[2]*Center for Cooperative Research on Alternative Energies (CIC energiGUNE), Basque Research and Technology Alliance (BRTA), Parque Tecnológico de Álava, 01510 Vitoria-Gasteiz, Spain*

Sulfide electrolytes including the argyrodite family (Li_6PS_5X, X = Cl, Br, I) exhibit high ionic conductivities and transference numbers and are regarded as promising electrolytes for all-solid-state lithium batteries. Although high ionic conductivity is a necessary requirement for feasible battery operation, other parameters are equally important and have often been neglected in efforts to realize all-solid-state batteries. The so-called critical current density (CCD) is among the more relevant parameters for application and indicates the maximum current an electrolyte can sustain before breakdown. When Li metal electrodes are used, this breakdown is often initiated by heavy dendrite formation and subsequent growth through the electrolyte layer, resulting in internal shorting of the cell. Very promising CCD values are reported for the argyrodite family of >1 mA cm^{-2} at elevated temperatures and pressures. However, non-standardized cell setups and testing procedures are employed, which renders a proper comparison of values impossible. Thus, this work investigates the impact of these often-overlooked parameters and aims at establishing more standard measurement procedures for solid electrolytes under ambient or almost ambient pressure. Furthermore, an alternative method for evaluation of CCD values is presented adopted from Tafel analysis.
 [DOI: 10.1149/1945-7111/ad01e3]

Manuscript submitted August 10, 2023; revised manuscript received September 6, 2023. Published October 20, 2023.

Supplementary material for this article is available online

Sulfide electrolytes including the argyrodite family (Li_6PS_5X, X = Cl, Br, I) are seen as one of the more promising materials regarding the development of solid-state batteries for the automotive sector.[1–4] With ionic conductivities which surpass even the ones for liquid electrolytes[5,6] they promise fast charging rates,[7] apart from high energy densities, and increased safety.[2,6] Furthermore, the low ecological footprint and abundant raw materials make them a rational choice in the race for applicable solid electrolytes.[1,8–10]

While high ionic conductivity is a necessary property of solid electrolytes, several other parameters are equally important. This is especially evident when the development of solid-state batteries towards commercialization is regarded. Apart from an abundant number of available solid electrolytes with high ionic conductivities >1 mS cm^{-2},[11] only a handful of these are employed in industry. One important parameter is the capability to prevent Li dendrite formation. In order to surpass the energy densities of conventional lithium-ion batteries using liquid electrolytes, Li metal electrodes need to be employed as anodes. This is especially true for solid-state batteries, as the higher density of solid electrolytes compared to liquid ones, imposes a major drawback regarding the achievable specific energies.[12] However, the use of Li metal electrodes poses the risk of short circuiting the battery during operation by growth of dendrites through the electrolyte layer.[13]

Thus, the race for higher ionic conductivities makes room for other parameters to become the focus of current research efforts. The so-called critical current density (CCD) is among the more relevant parameters and indicates the maximum current an electrolyte can sustain, before breakdown.[14–16] Usually, this point is indicated by an internal short of the used electrochemical cell, which is induced by heavy lithium dendrite formation. The dendrites grow through the electrolyte layer and once in contact with the opposite electrode, shorting of the cell occurs. Recently, a strong focus has been put on the CCD as it determines the maximum charge/discharge rate of a battery cell and acts as a good indicator for the applicability of the tested material for high power applications (e.g. automotive or aeronautic industry[15]).

In literature, though, a wide variety of CCD values are reported for the same material.[17] This is especially true for sulfide-electrolytes[14,18] and makes a meaningful prediction of battery cell performance impossible. Very promising CCD values for solid electrolytes are often obtained using very demanding measurement conditions. High pressures of several tens to hundreds of MPa and/or elevated temperatures[19–21] often present a distorted picture of the capabilities of sulfide electrolytes and impede a proper comparison with other electrolyte systems such as polymers or oxide-ceramics, which are usually tested under ambient conditions. Recent reports also indicate that the applied pressure during Li plating/stripping has a pronounced impact on the kinetics, such as nucleation, of the electrochemical reaction.[16] This indicates that more attention needs to be put on the measurement conditions for testing of new materials. Therefore, performance evaluations of emerging electrolytes for solid-state batteries are required to be conducted at more relevant conditions, at best ambient ones.

Furthermore, no standardized measuring procedures exist to evaluate CCD values. Conventionally, the electrolyte is sandwiched between two metallic Li electrodes and step chronopotentiometry is performed, i.e. a constant current is applied for a specific time and Li is either plated or stripped from the electrode surfaces.[15] Then the potential is reversed, and the plating/stripping reactions occur at the corresponding opposite electrodes. The current is further stepwise increased until an internal short or high polarization of the electrochemical cell is observed. The main parameters for such measurements are i) the time for which a constant current is applied and ii) the number of cycles for each current step.[15] However, a lot more experimental parameters can have a significant impact on the measurements. These are less evident and often not reported, reducing the reproducibility of results. Contact issues between the electrode and the electrolyte are one of the main challenges for reaching high CCD values.[16] Thus, experimental parameters like the used cell setup, the quality of the Li electrodes, and the thickness of the electrolyte layer can have a direct influence on the CCD measurement and need to be carefully considered.

Therefore, in this work, the impact of these *hidden* parameters on CCD measurements are investigated using the argyrodite electrolyte Li_6PS_5Cl as a model compound. Furthermore, an alternative method

[z]E-mail: alexander.beutl@ait.ac.at

for evaluating CCD values is elaborated based on galvanodynamic polarization adopted from Tafel analysis. This method yields more insight into the reaction kinetics of the electrochemical cell and allows for a more accurate analysis of the investigated material.

Experimental

Materials and cell assembly.—Commercially available fine Li_6PS_5Cl powder was purchased from NEI Corp. and used as received. Metallic lithium was purchased either as chips (MTI, 15.6 mm diameter, 0.25 mm thickness), or foil (Goodfellow, 38.1 mm width, 0.20 mm thickness) and will be further referred to as *Li chip* and *Li foil* respectively. Additionally, Li on Cu foil was purchased from China Energy Lithium Co., Ltd. (80 mm width, thickness of Li 0.04 mm) and will be referred to as *Li on Cu*. The Li chips and Li foil were cleaned prior usage by scratching off the surface layers using a scalpel. Subsequently, the cleaned lithium was further rolled in-between two pouch foils (Dai Nippon Printing, D-EL408PH(3)S-250) using a glass cylinder. Thus, cleaned, and smooth surfaces were obtained. Finally, electrodes of 8 mm diameter were cut from the prepared lithium using a manual punch. The Li on Cu was used as received.

For the CCD measurements, Li|Li symmetric cells were assembled using densified electrolyte pellets. These were prepared as follows: around 100 mg of the Li_6PS_5Cl powder was used and placed in a 10 mm hardened steel die set (Across International, W18Cr4V hardened carbon tool steel). Around 50 MPa were applied for a couple of seconds and then the pressure was increased to 360 MPa for 2 min. Dense pellets with densities in the range of 1.6 to 1.55 g cm^{-3} could be thus obtained, in good agreement with literature values and the crystallographic density of 1.64 g cm^3.[22]

For cell assembly three different cell setups were used, i.e. CR2032 coin cells (X2lab, SS316), ECC-Std (EL-CELL), and Swagelok cells (S4R, ½ inch diameter). They will be further referred to as CR2032, ECC-Std, and Swagelok setups, respectively. For assembly of CR2032 and ECC-Std cells, the Li electrodes were placed onto steel spacers (SS316, 15.5 mm diameter, 0.5 mm thickness) if not otherwise stated. CR2032 cells were assembled using a wave-shaped spring (1.5 × 1.4 mm). ECC-Std cells were assembled according to the information provided by the manufacturer using the conventional components. For Swagelok cells, the Li electrodes were directly put on the two steel plungers (SS316, ½ inch diameter) of the cells and further assembled by pushing the two plungers together and tightening the nuts. The used spring was contracted to a maximum unless otherwise stated. An image of the used cell setups is provided in the Supplementary (cf Fig. S1).

Electrochemical testing.—The CCD was measured using different measuring procedures. Step chronopotentiometry using one cycle per applied current step was performed. Current steps of 0.01 mA cm^{-2}, 0.02 mA cm^{-2}, 0.05 mA cm^{-2}, 0.10 mA cm^{-2}, 0.20 mA cm^{-2}, 0.50 mA cm^{-2}, 1.00 mA cm^{-2}, and 2.00 mA cm^{-2} were used. After each plating/stripping cycle a potentiostatic impedance measurement (PEIS) was conducted to verify possible short circuiting of the cells by dendrite formation. The PEIS was conducted from 1 MHz to 0.1 Hz using an AC excitation voltage of 50 mV.

Additionally, galvanodynamic polarization (or programmed current chronopotentiometry) was conducted. A linearly increasing current was applied to the sample cells starting from 0.01 mA cm^{-2} and ending at to 2 mA cm^{-2}. A current sweep rate of 0.20 μA $cm^{-2}s^{-1}$ was applied unless otherwise stated. PEIS measurements were conducted before and after the galvanodynamic polarization.

Scanning electron microscopy (SEM).—A ZEISS Supra 40 electron microscope was used for all measurements. Acceleration voltages of 3 kV were applied. Sample preparation was done inside an Ar-filled glovebox. Carbon pads were used for placing the sample on the respective holders. They were further put into a sealed container and transported to the microscope. The container was opened only for mounting the samples on the instrument, which prevented contamination of the samples.

Solid-state nuclearmagnetic resonance (ssNMR).—ssNMR was applied to determine the mobility of Li^+ on Li_6PS_5Cl solid electrolyte as well as to corroborate the presence of Li metal. ssNMR rotors were loaded with the solid electrolyte that has been previously plated/stripped until the cell short circuited. After cycling the cell, the Li electrodes were removed, and the outermost interfacial layer was scratched by a scalpel prior to pulverizing the pellet in powder. ssNMR experiment was recorded at a WB 500 MhZ Bruker Advance III spectrometer equipped with a 2.5 mm probe. Experiment was conducted spinning at the magic angle (MAS) at a frequency of 20 kHz and 1D 7Li spectra was obtained using single excitation pulses and recycling delays of 30 s.

Results and Discussion

Measuring procedure.—For the evaluation of CCD values, symmetric Li|Li cells are used, and metallic Li is plated/stripped from the electrodes at increasingly higher current densities. Eventually, dendritic lithium forms and grows throughout the solid electrolyte layer, shorting the working and counter electrodes. Thus, the electrochemical cell breaks down and the experiment is finished. The CCD is further identified as the maximum current density applied to the cell before this breakdown.[15] The increase of the current density can be done either stepwise (step chronopotentiometry) or continuously (galvanodynamic polarization). For the former two critical parameters can be identified[15] which have a stark influence on the obtained CCD values. (i) The amount of plating/stripping cycles applied at each current step and (ii) the time for which the current is applied during plating/stripping. For the latter the time can be kept constant for all current steps (*time-control*) or it can vary to keep the amount of charge deployed to the cell constant (*charge-control*). Depending on the selected parameters, the obtained CCD value might change significantly.

Symmetric Li|Li_6PS_5Cl|Li cells using *CR2032* setups and *Li chips* were assembled and tested using step chronopotentiometry. First plating/stripping cycles of one hour were used and only one cycle was applied at each current step. Then the number of cycles was increased to three and five. In addition, a *charge-control* measurement applying a constant charge of 1 mAh at each current step was performed. The results are depicted in Figs. 1 and S2.

The *time-control* step chronopotentiometry experiment using only one cycle at each current showed stable plating/stripping of Li metal up until current densities of 0.05 mA cm^{-2}. At 0.1 mA cm^{-2} the potential increases during the plating/stripping step, however, the cell does not short. At 0.2 mA cm^{-2} the overpotential increases sharply with time, but still no internal short by dendrites could be detected. Only at current densities of 0.5 mA cm^{-2} an internal short of the cell was recorded, indicated by a sharp decrease of the overpotential. The overpotential did not fall all the way to 0 V, though, indicating soft shorting of the cell. Following the suggestions from[15] PEIS measurements of the cells after each cycle were conducted (cf Fig. S3) and shorting of the cell could be verified by a stark drop in the impedance response after polarization at 0.50 mA cm^{-2}. The short circuiting of the cell was also corroborated by ssNMR where an additional signal of ^{7}Li at ca. 263 ppm could be observed in Fig. S4. The broad signal at 263 ppm can be ascribed to Li metal from the Li dendrite propagation generated during the plating/stripping measurements.

For the *time-control* measurements using multiple cycles of three and five at each current step, a similar trend as with one cycle could be observed. The major difference, though, was that shorting of the cell already occurred at lower current densities of 0.20 mA cm^{-2}. The *charge-control* measurement again showed an even lower CCD value. The cell shorts already at current densities of 0.10 mA cm^{-2}.

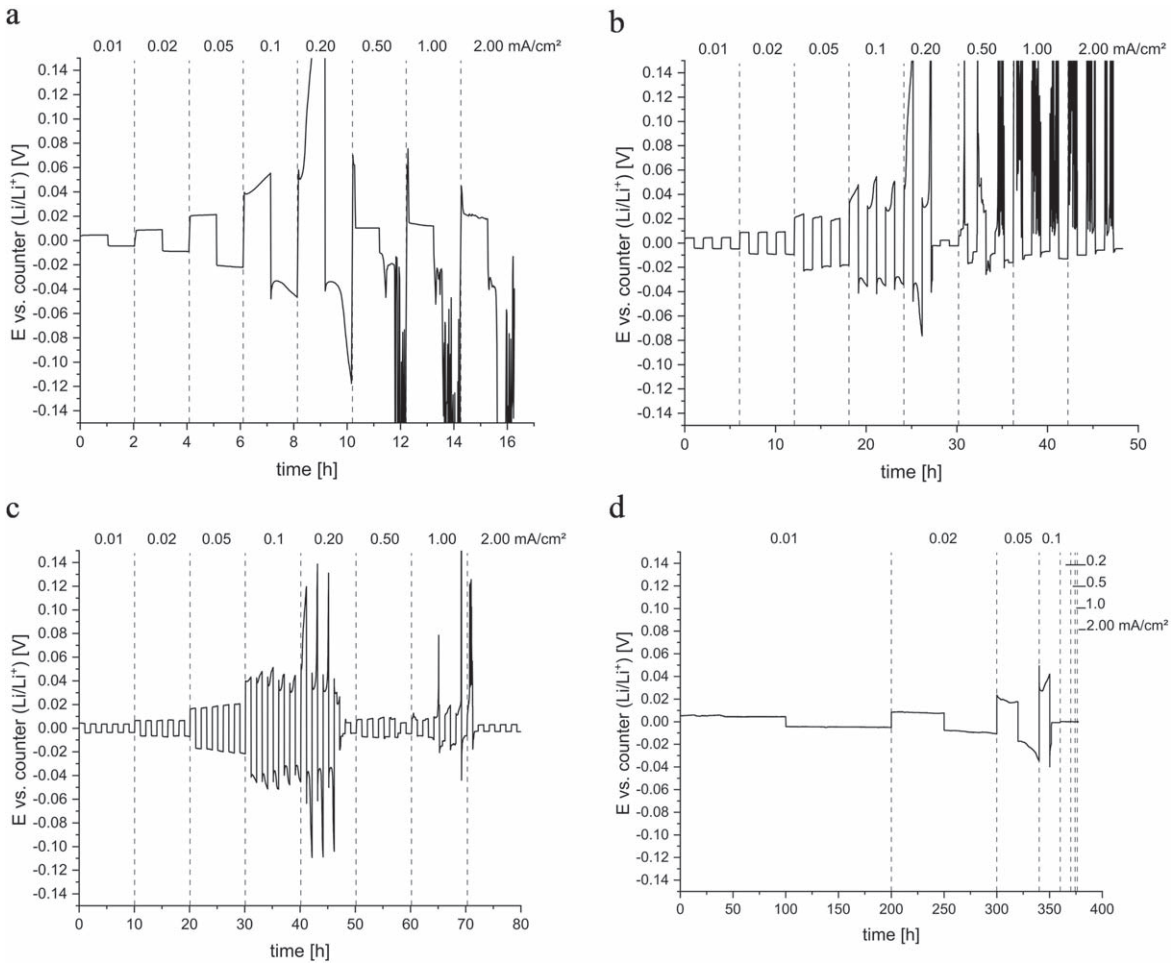

Figure 1. Step chronopotentiometry of LilLi$_6$PS$_5$ClILi cells using, (a), time-control (1 h) (b), multiple cycles (3 cycles, 1 h), (c), multiple cycles (5 cycles, 1 h), (d), charge-control (1 mAh). The plots depicted in (a), (b), are cut-outs of the corresponding complete plots in Fig. S2. The axes were scaled for ease of comparison.

When the potential profiles are regarded, a stable plateau is obtained up to 0.05 mA cm^{-2} for all measurements. At 0.10 mA cm^{-2} an irregular shaped potential profile, which is even more pronounced at 0.20 mA cm^{-2}, already indicates heavy lithium dendrite formation.[23] For the *time-control* measurements, the applied charge at 0.10 mA cm^{-2} amounts to only 0.10 mAh for each plating/stripping step. The current is reversed already before the Li dendrites can grow through the electrolyte layer which is rather thick at around 0.80 mm. When longer polarization steps are applied, as it is the case for the *charge-control* measurement, enough charge is applied at each step and Li dendrites can grow through the entire electrolyte layer. Similarly, when long cycling is applied (e.g. measurements using 3 or 5 plating/stripping cycles) at current densities beyond the CCD, lithium dendrites grow from both electrodes towards the center of the electrolyte layer and eventually short the cell. Long cycling measurements using *time-control* showed that it took 11 cycles at 0.10 mA cm^{-2} (applied for 1 h) until an internal short occurred (cf Fig. S5). As 0.10 mAh were applied at each cycle, a similar amount of charge was required to short the cell compared to the *charge-control* measurement. This finding is in good agreement with the concept of Sand's capacity introduced by Bai et al.,[24] which is calculated from Sand's time and the applied current density.

For evaluation of CCD values, *charge-control* measurements using reasonably high charge values ($\geqslant$1 mAh), seem to yield the most relevant results. A low CCD value which lies in the range of 0.05–0.10 mA cm^{-2} could be determined for Li_6PS_5Cl. For higher resolutions in the CCD values, more current steps with smaller increases in the current density need to be applied. This, however, will increase the time of the measurement significantly.

Unfortunately, step chronopotentiometry does not provide any information on the underlying bottlenecks of the electrochemical process and no rational strategy for enhancing the critical current density can thus be elaborated.

Therefore, another approach for determining the CCD by galvanodynamic polarization (or programmed current chronopotentiometry) was adopted from conventional Tafel analysis. Similar to step chronopotentiometry a current is applied to the cell and the potential response is recorded. However, the current is continuously increasing, rather than step-wise. The proposed method relates to conventional Tafel analysis, and the recorded potential follows the Butler-Volmer equation.[25,26] At high currents, i.e. far from the equilibrium state, the overpotential increases sharply and the classic Tafel behavior is observed (i.e. logarithmic relation between i and η). In this region, the applied current usually lies beyond the diffusional limit of the electrolyte and unstable Li plating, i.e. severe dendrite formation, is observed.[24] The Li^+ concentration at the electrode surface is almost zero and diffusion of the ions from the bulk electrolyte is the rate determining step. At intermediate current densities below the Tafel regime, the Li^+ concentration at the electrode surface starts to deplete at the beginning of polarization and reaches zero only at a characteristic time governed by Sand's equation.[24,27] Depending on the applied current density, more or less charge can be applied to the system before dendrite formation starts. Thus, only for low current densities, below the diffusional limit of

the electrolyte, stable Li plating can occur, even for prolonged times and the risk of shorting the cell by Li dendrites penetrating through the electrolyte layer is minimized. At low currents, i.e. low overpotentials, the exponential terms of the Butler-Volmer equation can be approximated and a linear increase of the overpotential with applied current can be observed according to Eqs. 1, 2.[25,28,29]

$$i = -i_0 f\eta \quad [1]$$

$$R_{ct} = \frac{RT}{Fi_0} \quad [2]$$

The negative reciprocal slope of the η vs i plots further corresponds to the charge transfer resistance (R_{ct}) and indicates the kinetic facility of the electrochemical reaction. For very high reaction rate constants, R_{ct} approaches 0.

Thus, in focusing on the low current density region of the galvanodynamic polarization measurements, the critical current density can be identified as the end of the linear region of the i vs η plots. Furthermore, the R_{ct} can be derived from the slope of these plots and gives insights into possible contact issues between the electrode and electrolyte. A schematic of the different regions in galvanodynamic polarization curves as well as the evaluation of the CCD is shown in Fig. 2a.

Stable lithium plating/stripping can only be ensured for current densities which lie in the linear regime. For this range, the Li^+ diffusion is fast enough to avoid ion-depletion at the electrode surface and thus uncontrolled dendrite formation.[24] At higher current densities in the Tafel regime, Li^+ ions are already depleted at the electrode surfaces and a continuous concentration gradient is formed throughout the electrolyte. In the Sand regime, the Li^+ ions at the surface of the electrodes are not yet depleted, however, according to Sand's equation,[24,27,30] will deplete over time. Therefore, the onset of Sand's regime and the end of the linear regime of the galvanodynamic polarization indicate the CCD for the studied material. In addition, by evaluating R_{ct} and i_0, more insight into the reaction kinetics is provided and possible bottlenecks for the Li plating/stripping reactions can be identified. Especially i_0 can give insights into the stability of the Li stripping process as reported recently.[31]

For the galvanodynamic polarization three parameters are relevant, (i) the current at the beginning of the measurement, (ii) the current at the end of the measurement, and (iii) the sweep rate. The influence of the latter one on the obtained CCD values was experimentally evaluated. The current limits were set at 0.01 mA cm^{-2} and 2 mA cm^{-2} whereas different sweep rates of 2.00 μA $cm^{-2}s^{-1}$, 0.20 μA $cm^{-2}s^{-1}$, and 0.02 μA $cm^{-2}s^{-1}$, were applied. Symmetric Li|Li_6PS_5Cl|Li cells using *CR2032* casings and *Li chips* were assembled and tested. The results are depicted in Figs. 2b–2d and Table I.

R_{ct} were determined by evaluating the slope of a linear function which was fitted to the data at low current densities. CCD values

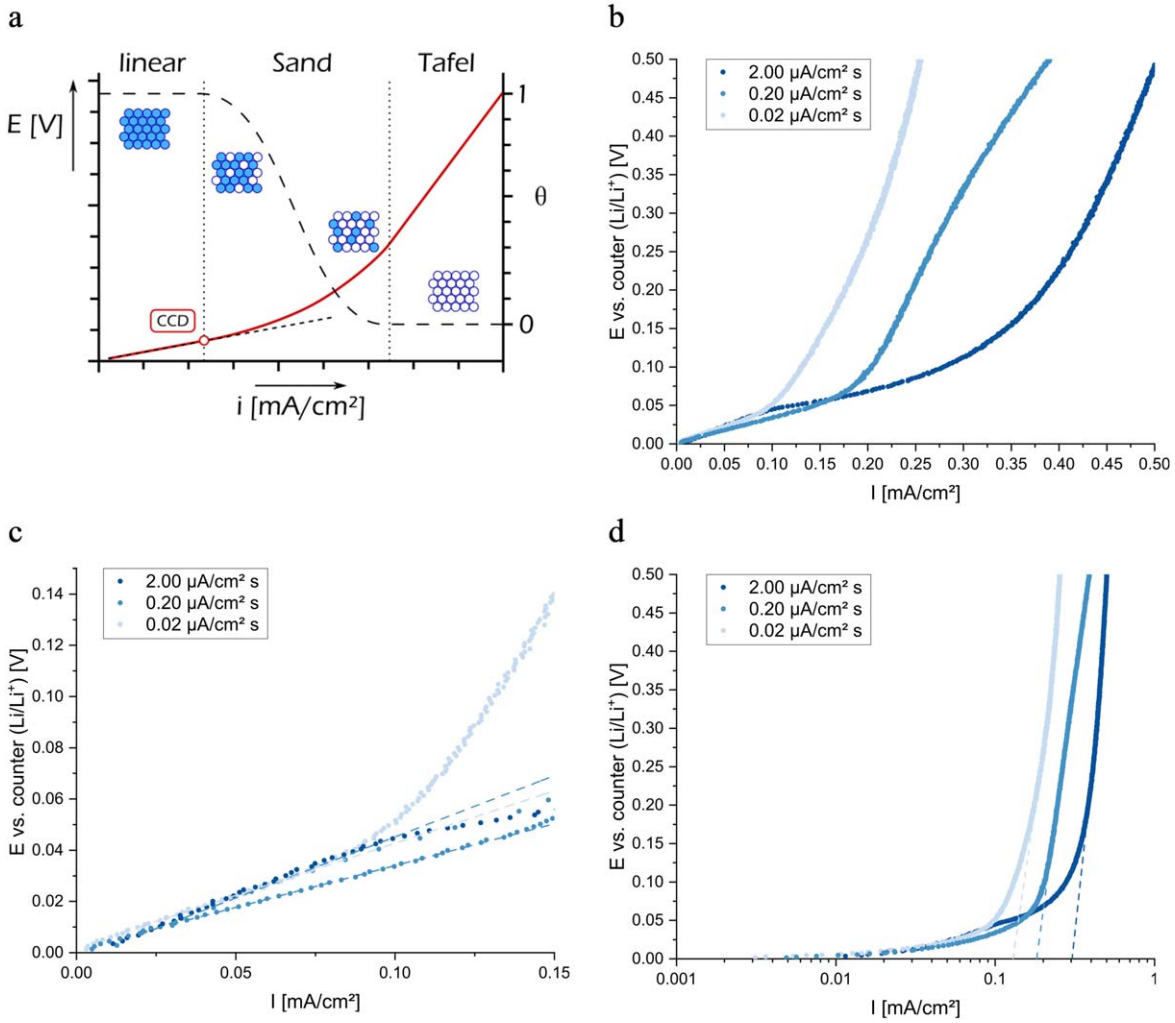

Figure 2. (a), schematic outline of the different regions of the galvanodynamic polarization measurements. In addition, the surface coverage (θ) of the electroactive species is plotted with dashed lines; (b), CCD measurements using galvanodynamic polarization at different sweep rates; (c), enlarged view on the linear regime of the measurements depicted in (b), (d), Tafel plot of the measurements depicted in (b).

Table I. Apparent exchange current densities (j_0), charge transfer resistances (R_{ct}), and CCD values obtained at different sweep rates.

sweep rate [μA cm^{-2} s]	j_0 [mA cm^{-2}]	R_{ct} [Ω]	CCD [mA cm^{-2}]
2.00	0.30	478	0.094
0.20	0.18	327	0.096
0.02	0.13	408	0.075

were further determined as the onset of the Sand regime, i.e. at the first deviation from linearity at lower current densities (cf Fig. 2c). Additionally, exchange current densities were obtained from fitting the log i vs η plots at higher current densities using a linear function. It's intercept with the *x*-axis corresponds to the exchange current density (cf Fig. 2d). Only the geometric surface area of the electrodes was used to calculate the current densities from the measured currents and thus surface roughness of the electrodes and/or the prepared Li_6PS_5Cl pellets are not taken into account. During the measurements, Li will be plated on one electrode and stripped from the other one, leading to a change in the surface area during the measurement. Therefore, the exchange current densities are considered as *apparent* exchange current densities (j_0) only.

The obtained R_{ct} of 478 Ω, 327 Ω, and 408 Ω are in good agreement with EIS measurements conducted before the galvanodynamic polarization and indicate slight differences in the contact between the Li metal electrodes and the Li_6PS_5Cl pellet. Slight deviations of the electrolyte and electrode thicknesses, which were in the range of 0.85–0.80 mm and 0.15–0.10 mm respectively could be the reason for this observation. Due to the static configuration of the CR2032 cell, small deviations in the sample sizes result in different internal pressures, which cannot be compensated.

Recently, it could be found that too high j_0 lead to interfacial instabilities during Li stripping and increased pore formation. This will eventually result in cell failure by internal short. Nevertheless, for exchange currents below 4 mA cm^{-2}, as was observed in this work, the influence of j_0 on the cell stability is only minor.[31,32] The j_0 obtained are directly proportional to the sweep rate and the highest value of 0.30 mA cm^{-2} is found for 2.00 μA cm^{-2} s^{-1}. This trend is in good agreement with reports[33,34] which found that at higher sweep rates higher double-layer charging effects are observed and concomitantly higher j_0 values are recorded. Thus, it was concluded, that rather low sweep rates or even galvanostatic conditions should be applied for such kind of measurements.[34–36] On the other hand, for lower sweep rates, more charge is applied to the system and thus more Li is plated on the working electrode. As the morphology of the plated Li creates a high surface area, the measured apparent current density using the geometric area of the electrode deviates more and more from the real current density. For the measurements using 0.02 μA cm^{-2}s^{-1}, 0.20 μA cm^{-2}s^{-1}, and 2.00 μA cm^{-2}s^{-1} a total charge of around 4.00 mAh, 0.40 mAh, and 0.04 mAh is applied. Consequently, too low sweep rates should also be avoided. Therefore, sweep rates of 0.20 μA cm^{-2} are applied for all further measurements.

The CCD values lie in the range of 0.075 mA cm^{-2} to 0.096 mA cm^{-2} and are comparable to the findings obtained from the step chronopotentiometry measurements. The good agreement of the measuring procedures is readily depicted in Fig. S6. The increase of the overpotential with current density is similar for both methods. When the current densities go beyond the CCD value of around 0.1 mA cm^{-2} though, the slope of di/dE in the galvanodynamic polarization measurements deviates from linearity, whereas an increase in the overpotential with time is observed for the step chronopotentiometry measurements. This shows that shorting of the cell by dendrite formation seems to be an inappropriate indicator for the CCD value and the increase in the overpotential is more reliable.

The rather low CCD values of around 0.1 mA cm^{-2} obtained under ambient conditions in this work compared to reported values of 0.3–2.15 mA cm^{-2}[14] show the significant influence of the experimental parameters on the resulting CCD. Low stack pressures and concomitant poor interfacial contact between the electrodes and electrolyte layers result in a reduced CCD. Recently, it was found that pore formation during Li stripping is increased at stack pressures below 5 MPa and current densities just above 0.5 mA cm^{-2} for solid electrolytes[31] could be obtained. This trend is also observed for the samples measured in this work. Applying increased pressures during the CCD measurements, results in higher values 0.3–2.15 mA cm^{-2}, as reported earlier.[14]

The obtained j_0 are quite sensitive to a change in the sweep rate and range from 0.13–0.30 mA cm^{-2}. They are considered as an indicator for the rate constant of the electrochemical reaction. Recently, it could be found, though, that too high j_0 values lead to interfacial instabilities during Li stripping and increased pore formation. This will eventually result in cell failure by internal short. Nevertheless, for exchange currents below 4 mA cm^{-2} the influence of j_0 on the cell stability is only minor.[31,32]

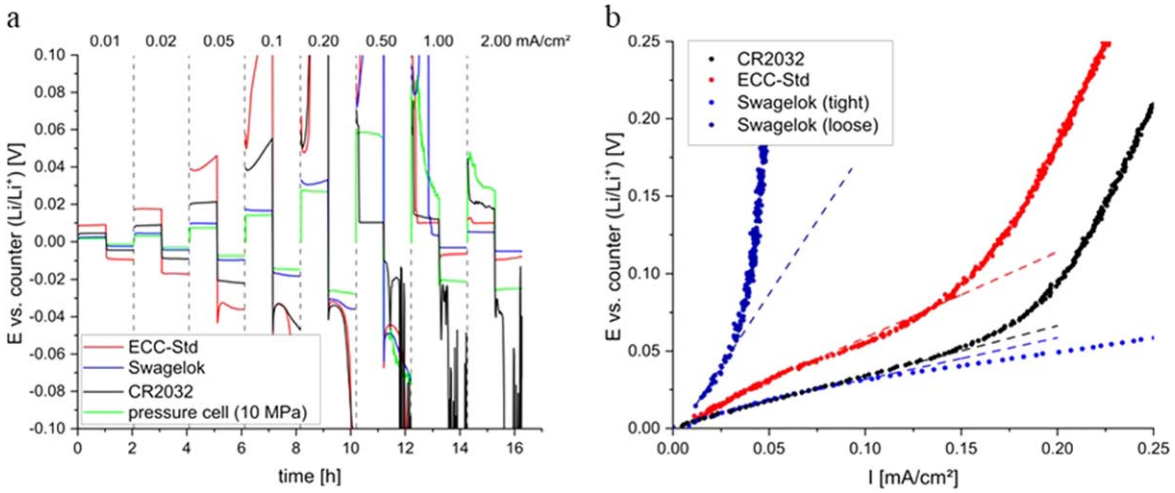

Figure 3. CCD measurements conducted in different electrochemical cell setups, (a), step chronopotentiometry, and, (b), galvanodynamic polarization were applied. For the latter, the linear region is fitted with dashed lines.

Table II. Apparent exchange current densities (j_0), charge transfer resistances (R_{ct}), and CCD values obtained for different cell setups.

Cell setup	j_0 [mA cm^{-2}]	R_{ct} [Ω]	CCD [mA cm^{-2}]
ECC-Std	0.16	653	0.062
CR2032	0.18	327	0.096
Swagelok (tight)	0.38	269	0.115
Swagelok (loose)	0.042	1988	0.035

Measuring setup.—A wide spread of different CCD measurements is observed in literature for the same material. Especially for dry solid electrolytes used for battery applications this is a severe issue[37] as often non-commercial *home-made* measuring setups are used. The cell setup used for CCD measurements has a profound influence on the obtained data as it defines the applied pressure on the samples during the measurement. As reported in Ref. 14 already small changes in the applied stack pressure can induce significant differences in the obtained CCD values.

To further elucidate the impact of the cell device, three different commercially available electrochemical cells were employed to measure the CCD of Li|Li_6PS_5Cl|Li cells. Both, step chronopotentiometric and galvanodynamic polarization procedures were applied; the results are shown in Fig. 3 and Table II.

Samples measured by galvanodynamic polarization showed CCD values of 0.062 mA cm^{-2}, 0.096 mA cm^{-2} and 0.115 mA cm^{-2}, and R_{ct} of 653 Ω, 478 Ω, and 334 Ω for ECC-Std, CR2032, and Swagelok cell setups, respectively.

For step chronopotentiometry, the same trend was observed with the sample in the Swagelok setup showing the lowest overpotential for all current steps. The poorest performance was observed for the ECC-Std, showing high overpotential for each current step. Already at 0.1 mA cm^{-2} the potential increases strongly. However, shorting of the cell is only observed at a current density of 1.00 mA cm^{-2}. Thus, a rather high CCD value is obtained for the ECC-Std setup, although heavy dendrite formation is expected already before 1.00 mA cm^{-2} as indicated by the increase in the plating/stripping potential. Shorting of the cell occurs only at 1.00 mA cm^{-2}, which was confirmed by PEIS measurements after the corresponding plating/stripping cycles (cf Fig. S7). In the Swagelok setup the step chronopotentiometry showed stable cycling up to 0.20 mA cm^{-2}. At 0.50 mA cm^{-2} the overpotential increases sharply and shorting of the cell due to dendrite formation occurs at 1.00 mA cm^{-2}. Similar CCD values were obtained for the ECC-Std setup and the Swagelok cell, although quite different overpotentials were observed during plating/stripping cycles. The different CCD values obtained for the ECC-Std cell from the step chronopotentiometry and galvanodynamic measurements shows that it is difficult to accurately determine the CCD and depending on the definition of this parameter (indicated by shorting of the cell or by an increase in the slope of the η vs i plot) the values might vary strongly.

The higher CCD value for the Swagelok cell could also be confirmed by long cycling measurements. Symmetric cells using Li metal electrodes were assembled in CR2032 and Swagelok cells. Both cells were cycled at 0.10 mA cm^{-2} using one hour plating/stripping steps. It can be seen in Fig. S5 that the CR2032 cell showed an internal short already after 22 h, whereas the Swagelok cell continued cycling well beyond 100 h.

In order to further validate the results, two further experiments were conducted. First, an experimental pressure cell[38] was used to measure the CCD at 10 MPa to depict the impact of pressure on the obtained CCD values. Step chronopotentiometry was conducted and the results are shown in Fig. 3. The higher pressure could effectively decrease the required overpotential for plating/stripping of Li metal, and stable current profiles could be obtained up to 0.20 mA cm^{-2}. Indeed, the increased pressure improved the stripping/plating behaviour of the cell and increased the observed CCD. The second experiment was conducted using a Swagelok cell, however, the spring was only slightly compressed. Then galvanodynamic polarization was applied (cf Fig. 3). The loose spring resulted in high R_{ct} and low CCD of 1988 Ω and 0.035 mA cm^{-2}, respectively. The high dependence of the CCD values on the applied pressure, demands to control this parameter properly to obtain reproducible results.

Thus, the stack pressure for the used cell setups was determined using, a conventional peel tester. The load required to fully close/compress the cells was measured. The spring of the Swagelok cell is fully compressed during cell assembly and thus directly determines the applied stack pressure. When the cell is compressed using the peel tester, the load can be measured and a linear dependency of the displacement with the applied load is observed in good agreement with Hooke's law (cf Fig. 4).

When the cell is fully compressed, the load sharply increases, and further displacement is negligible. Thus, the spring constant can be determined by fitting the linear region of the load vs displacement plots and the stack pressure is obtained from the onset of the sharp increase in load. For the Swagelok cell a spring constant of 2.0 N mm^{-1} and a stack pressure of 10 N was determined. For an electrode area of 0.5 cm^2 an internal pressure of 0.20 MPa can be derived from these values. Similar measurements were conducted for

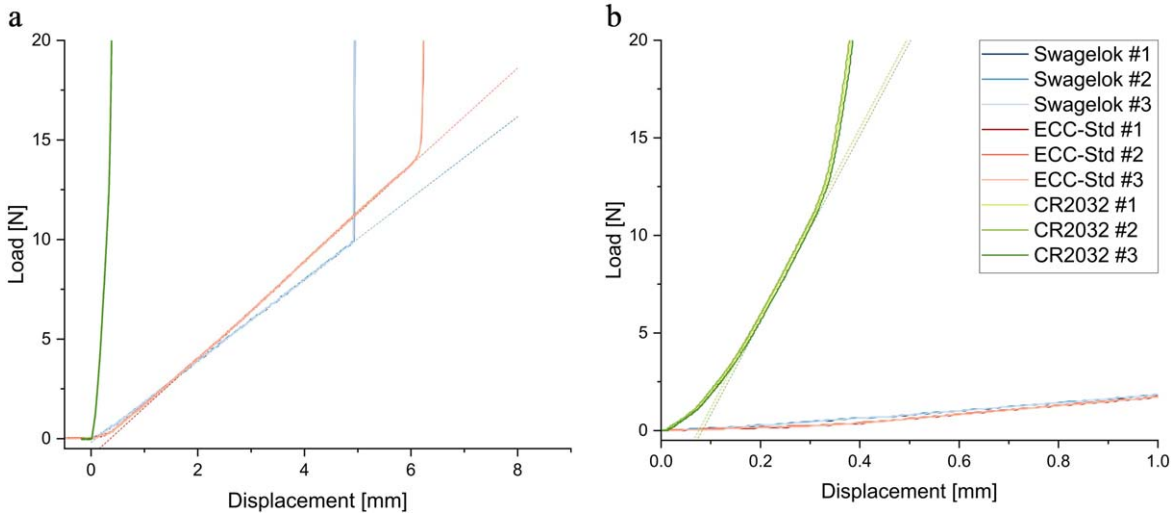

Figure 4. Load vs displacement graph for measuring the pressure inside the different cell setups. The spring constant of the used springs was determined by fitting the linear region of the plots (dashed lines).

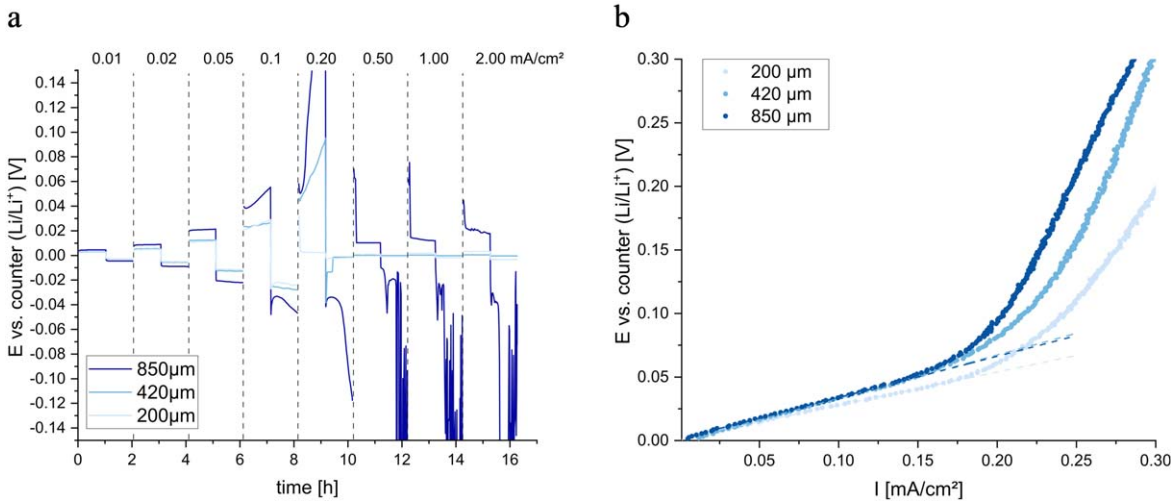

Figure 5. (a), Step chronopotentiometry and (b), galvanodynamic polarization measurements in *CR2032* coin cells using electrolyte pellets with different aspect ratios (diameter:thickness).

Table III. Apparent exchange current densities (j_0), charge transfer resistances (R_{ct}), and CCD values obtained for different cell setups.

Electrolyte thickness [mm]	j_0 [mA cm^{-2}]	R_{ct} [Ω]	CCD [mA cm^{-2}]
0.85	0.18	327	0.096
0.42	0.19	341	0.127
0.20	0.20	261	0.117

Table IV. Apparent exchange current densities (j_0), charge transfer resistances (R_{ct}), and CCD values obtained for different lithium sources.

Lithium source	Apparent j_0 [mA cm^{-2}]	R_{ct} [Ω]	CCD [mA cm^{-2}]
Li chip	0.18	327	0.096
Li foil	0.21	323	0.154
Li on Cu	0.31	305	0.194
Li chip (as received)	0.07	2073	0.023

the ECC-Std cell; however, a 1.9 mm spacer was added to replace the sample setup consisting of (spacer|Li|Li_6PS_5Cl|Li|spacer). Here a spring constant very similar to the one for the Swagelok cell could be observed of 2.2 N mm^{-1} and a stack pressure of 14 N, corresponding to an internal pressure of the cell of 0.28 MPa. For the CR2032 setup, again a 1.9 mm spacer was added for measuring the internal pressure of the cell. A rather high spring constant of 43.1 N mm^{-1} was recorded and a stack pressure of 12 N, corresponding to an internal pressure of 0.24 MPa.

The rather similar stack pressures of 0.20–0.28 MPa inside the different cell setups cannot explain the differences obtained in the CCD measurements. Therefore, other parameters need to be regarded to explain the observed differences. One potential explanation for the improved CCD values obtained in Swagelok cells could be the different cell assembly procedure. During cell assembly the Swagelok cell needs to be manually compressed tightly before tightening the nuts. In this step, high pressure can be applied to the cell, resulting in better contact between the electrode and electrolyte layers. This could have a significant impact on the measurements, which needs to be further explored.

Electrolyte thickness.—CCD measurements of solid electrolytes using thick powder pellets are often regarded as non-representative as very thin electrolyte films need to be employed for practical application.[9,39]

Therefore, the thickness of the electrolyte layer was reduced from 0.85 mm to 0.42 mm and 0.20 mm. A *CR2032* setup was used for all samples. To enable comparable pressure in all cells, the decrease of the sample thickness was compensated by addition of more steel spacers in the cell. The results are shown in Fig. 5 and Tables III and IV.

All cells show similar CCD and R_{ct} in the galvanodynamic polarization curves, verifying similar interfaces for all cells. An increasing j_0 from thicker to thinner sample pellets, however, could be observed. This trend was already pointed out in Ref. 24, where the limiting current at which the overpotential increases rapidly was characterized as inversely proportional to the distance of the two electrodes, i.e. to the thickness of the electrolyte. For thinner electrolyte layers, the Li^+ ions need to cover less distance to reach the respectively other electrode, compared to thicker electrolytes. Therefore, the onset of the potential increase in Fig. 5 is at lower current densities for the thick electrolyte pellet (0.85 mm), whereas it is highest for the thin one (0.20 mm).

For the step chronopotentiometric measurements a similar behavior for all samples could be observed. An increased overpotential was recorded for the 0.85 mm sample due to the higher bulk resistance of the thick electrolyte pellet. At 0.20 mA cm^{-2} the overpotential increases strongly for the 0.85 mm electrolyte layer. Both, the 0.20 mm and 0.42 mm layer cells already short at this current density, with the latter one only during the second half of the polarization. Clearly thinner electrolyte layers are more susceptible to being penetrated by Li dendrites as the distance which needs to be covered by the growing dendrites to reach the opposite electrode is reduced. Therefore, a breakdown of the electrolyte

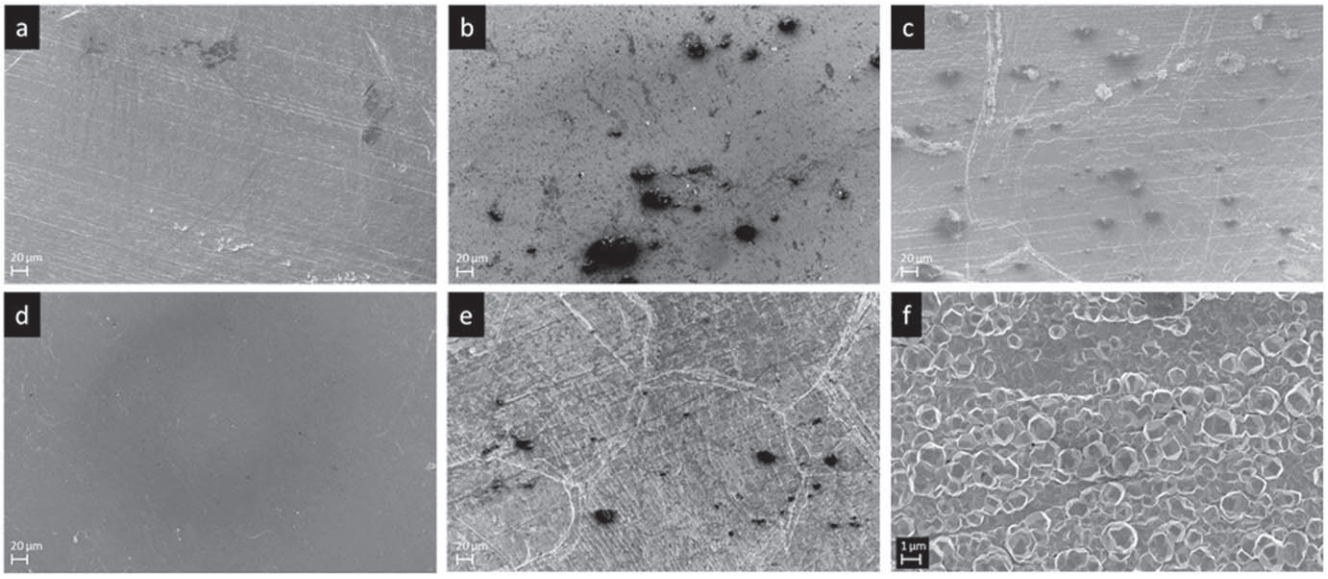

Figure 6. SEM micrographs of the different Li metal sources used as electrodes. (a)–(c), *Li chip*, *Li foil* and *Li on Cu* before cleaning, (d), (e), *Li chip* and *Li foil* after cleaning. (f), Cu current collector of the *Li on Cu* foil.

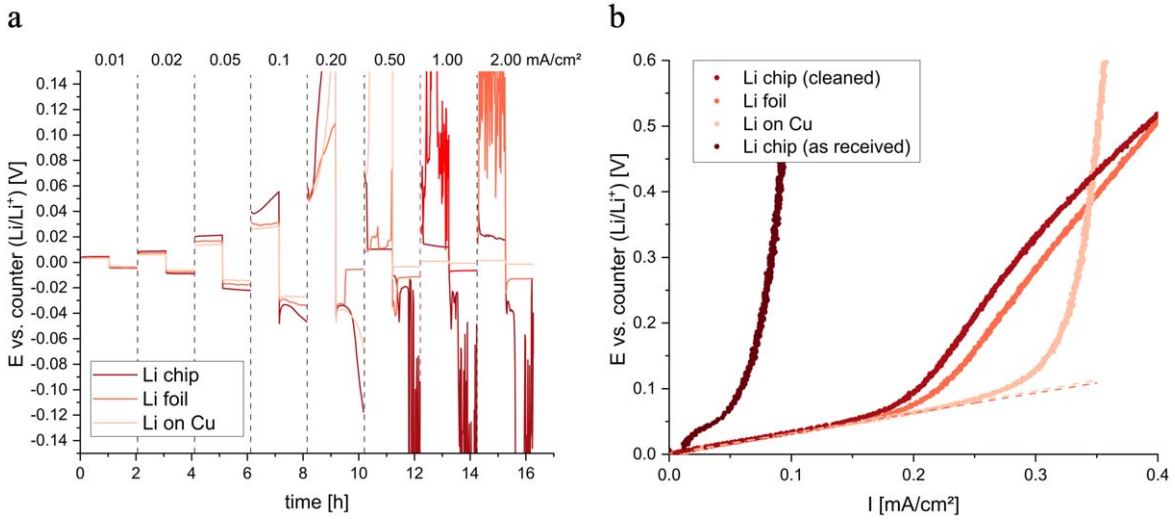

Figure 7. (a), step chronopotentiometry and (b), galvanodynamic polarization measurements in CR2032 cells using different Li sources.

results immediately in an internal short of the cell for samples using thin electrolyte layers. In comparison, the sample using 0.85 mm thick electrolyte layers only shorts at a current density of 0.5 mA cm^{-2}. Thus, for step chronopotentiometry a rather thin electrolyte layer should be used in order to avoid an overestimation of the stability. For galvanodynamic polarization, however, no dependence on the electrolyte thickness for the estimation of the CCD could be observed.

Li metal source.—Usually, thick lithium foils are used for application in pressure cells using sulfide-based electrolytes.[40] However, regarding application in real-world battery cells, a thin Li layer of only a few tens of μm should be employed to maximize the achievable energy density. Lithium metal comes in different forms and qualities. In order to investigate the influence of the used lithium electrodes on the obtained CCD, three different Li sources were applied, i.e. *Li-chips*, *Li-foil*, and *Li on Cu*.

Because of the high reactivity of metallic Li, a passivation layer is built up over time even when stored inside an Ar-filled glovebox.[41] Therefore, Li metal should be cleaned before usage. In this work, the Li was first cleaned by scratching off the uppermost layer using a scalpel and subsequently the surface was smoothed by rolling between two pouch foils. A mechanical cleaning process for thin Li metal layers deposited on Cu foil is not possible, as the Li layer would be destroyed during the procedure, leaving only the bare Cu foil. Therefore, such foils need to be stored in sealed pouch bags within a glovebox and should only be opened right before usage.[41] SEM micrographs of the different Li sources used are presented in Fig. 6. Clearly a lot of impurities can be seen on the Li electrodes before cleaning, whereas less impurities are visible after the cleaning step. For the Li on Cu foil, the Li was deposited on a rough Cu substrate and some impurities are observed at the surface.

The results of the CCD measurements are depicted in Fig. 7. The step chronopotentiometry showed stable plating/stripping cycles for all electrodes up to 0.05 mA cm^{-2}. At 0.10 mA cm^{-2} stable cycling is observed only for the sample using the *Li on Cu* electrodes. In contrast, samples using the *Li-foil* and *Li-chips* showed a slight to medium increase of the overpotential with time. At 0.2 mA cm^{-2} the overpotential of all samples increases significantly and the sample using the *Li-foil* shows even a short circuit.

The galvanodynamic polarization show similar R_{ct} of 324 Ω, 305 Ω, and 323 Ω, for the *Li chip*, *Li foil*, and *Li on Cu* electrodes, respectively. The j_0 as well as the CCD values show pronounced differences, though, when the cleaned electrodes (*Li chip* and *Li foil*) are compared with the *Li on Cu* electrode, which could not be cleaned prior to usage. The i vs E plots at higher current densities show far larger slopes for the *Li on Cu* sample compared to the ones using cleaned Li metal surfaces. The passivation layer on the non-cleaned sample changes the surface chemistry and thus surface diffusion of the Li^+ ions is altered. This will lead to higher resistances and concomitantly to higher overpotentials. The higher CCD values observed for the *Li on Cu* electrodes might be an effect from the observed impurities which can increase the electrode area significantly and thus decrease the effective current density. Assuming only a thin passivation layer, as the *Li on Cu* samples were stored inside a sealed pouch bag, the additional resistance is negligible.[41]

To verify this assumption, non-cleaned Li chips were also measured by galvanodynamic polarization. As expected, high R_{ct} and very low CCD and j_0 were obtained. Surprisingly though, the slope of the i vs E plot at high current densities resembles the one for the *Li on Cu* electrodes indicating the effect of surface impurities on the galvanodynamic polarization curves.

Conclusions

Summarizing, two different methods for the determination of critical current densities (CCD), namely step chronopotentiometry and galvanodynamic polarization, were compared for their robustness towards changes in the experimental setups. Similar values in the range of 0.1–0.2 mA cm^{-2} could be obtained from both measurement procedures. Galvanodynamic polarization is considered as the more powerful method, though, as it yields more insight into the kinetics of the electrochemical reaction. The R_{ct} as well as j_0 can be simultaneously obtained from one measurement and give important hints on how to enhance the CCD for a specific materials system.

Furthermore, the *hidden* parameters of CCD measurements, i.e. cell setup, electrolyte thickness and Li source were evaluated on their impact on the obtained values. The following conclusions can be drawn from this study:

- The employed measuring cell has a pronounced impact on the obtained CCD as different pressures are applied to the sample for different setups. When non-commercial (*home-made*) cells are used, proper characterization of the pressure being applied to the sample needs to be conducted in order to maintain reproducibility of the reported data. A higher pressure will yield enhanced CCD values, mainly due to the decrease of R_{ct}.
- The thickness of the electrolyte layer being employed in the CCD measurements did not show a significant influence on the obtained CCD values. For step chronopotentiometry thicker electrolyte layers will lead to an overestimation of the CCD as the Li dendrites need to cover a longer distance to short the cell. Thus, rather thin electrolyte layers should be used for the determination of CCD values by step chronopotentiometry. For the galvanodynamic polarization measurements, though, no significant impact of the sample thickness on the CCD values was observed.
- The used Li source, especially the passivation layers found on Li metal show a great impact on the CCD measurements. Thus, cleaning of Li electrodes prior to the measurements cannot be avoided. *Li on Cu* samples which were stored in a sealed pouch bag inside the glovebox, showed a passivation layer and a different potential response during galvanodynamic polarization, compared to cleaned Li chips and foils.

Regarding the applicability of Li_6PS_5Cl for battery application under ambient conditions it could be found that the high interfacial resistance is the main bottleneck for application. Usually, this issue is resolved in literature by application of high pressures during cycling of solid-state batteries.[19,42,43] This approach seems to be less feasible at larger scale and thus other approaches need to be developed to mitigate the issue. Soft interfacial layers between the electrodes and the sulfide electrolytes seem to be a promising approach to improve interfacial contact and thus reduce interfacial resistances. Similar approaches have been reported for other sulfide- and garnet type ceramic electrolytes and promising CCD values could be obtained.[11,44] This approach can enable stable cycling of solid-state batteries using sulfide electrolytes with metallic Li electrodes under ambient conditions.

Acknowledgments

The presented work was supported by the European Commission through the H2020 program under Grant agreement number 875028 (SUBLIME Project) and from the European Union's Horizon Europe program for research and innovation under grant agreement No. 101069686 (PULSELION project). Furthermore, the authors want to express their gratitude to Jacqueline Winter and Andrea Paolella for proofreading and corrections as well as Ningxin Zhang for SEM analysis.

ORCID

Artur Tron https://orcid.org/0000-0002-6565-8247
Alexander Beutl https://orcid.org/0000-0002-7098-619X

References

1. J. Schnell, T. Günther, T. Knoche, C. Vieider, L. Köhler, A. Just, M. Keller, S. Passerini, and G. Reinhart, *J. Power Sources*, **382**, 160 (2018).
2. J. Chen, J. Wu, X. Wang, A. Zhou, and Z. Yang, *Energy Stor. Mater.*, **35**, 70 (2021).
3. Y.-K. Sun, *ACS Energy Lett.*, **5**, 3221 (2020).
4. J. Wu, S. Liu, F. Han, X. Yao, and C. Wang, *Adv. Mater.*, **33**, 2000751 (2020).
5. W. G. Suci, H. Aliwarga, Y. R. Azinuddin, R. B. Styawati, K. N. R. Stulasti, and A. Purwanto, *Open Engineering*, **12**, 409 (2022).
6. L. Wang, J. Li, G. Lu, W. Li, Q. Tao, C. Shi, H. Jin, G. Chen, and S. Wang, *Sec. Energy Materials*, **7**, 111 (2020).
7. Y. Jin, Q. He, G. Liu, Z. Gu, M. Wu, T. Sun, Z. Zhang, L. Huang, and X. Yao, *Adv. Mater.*, **35**, 2211047 (2023).
8. D. Karabelli, K. P. Birke, and M. Weeber, *Batteries*, **7**, 18 (2021).
9. J. Schnell, H. Knörzer, A. J. Imbsweiler, and G. Reinhart, *Energy Technol.*, **8**, 1901237 (2020).
10. J.-L. Popien, C. Thies, A. Barke, and T. S. Spengler, *Int. J. Life Cycle Assess.*, **28**, 462 (2023).
11. F. Zheng, M. Kotobuki, S. Song, M. O. Lai, and L. Lu, *J. Power Sources*, **389**, 198 (2018).
12. T. Placke, R. Kloepsch, S. Dühnen, and M. Winter, *J. Solid State Electrochem.*, **21**, 1939 (2017).
13. Y. Takeda, O. Yamamoto, and N. Imanishi, *Electrochemistry*, **84**, 210 (2016).
14. S.-Y. Ham et al., *Energy Stor. Mater.*, **55**, 455 (2023).
15. Y. Lu, C.-Z. Zhao, H. Yuan, X.-B. Cheng, J.-Q. Huang, and Q. Zhang, *Adv. Funct. Mater.*, **31**, 2009925 (2021).
16. Y. Liang, H. Liu, G. Wang, C. Wang, Y. Ni, C.-W. Nan, and L.-Z. Fan, *InfoMat.*, **4**, e12292 (2022).
17. J. Peng, D. Wu, F. Song, S. Wang, Q. Niu, J. Xu, P. Lu, H. Li, L. Chen, and F. Wu, *Adv. Funct. Mater.*, **32**, 2105776 (2022).
18. H. Wan, Z. Wang, S. Liu, B. Zhang, X. He, W. Zhang, and C. Wang, *Nat. Energy*, **8**, 473 (2023).
19. D. K. Singh, A. Henss, B. Mogwitz, A. Gautam, J. Horn, T. Krauskopf, S. Burkhardt, J. Sann, F. H. Richter, and J. Janek, *Cell Reports Physical Science*, **3**, 101043 (2022).
20. F. Han, J. Yue, X. Zhu, and C. Wang, *Adv. Energy Mater.*, **8**, 1703644 (2018).
21. G. Liu, W. Weng, Z. Zhang, L. Wu, J. Yang, and X. Yao, *Nano Lett.*, **20**, 6660 (2020).
22. J.-M. Doux, H. Nguyen, D. H. S. Tan, A. Banerjee, X. Wang, E. A. Wu, C. Jo, H. Yang, and Y. S. Meng, *Adv, Energy Mater.*, **10**, 1903253 (2020).
23. K. N. Wood, E. Kazyak, A. F. Chadwick, K.-H. Chen, J.-G. Zhang, K. Thornton, and N. P. Dasgupta, *ACS Cent. Sci.*, **2**, 790 (2016).
24. P. Bai, J. Li, F. R. Brushett, and M. Z. Bazant, *Energy Environ. Sci.*, **9**, 3221 (2016).
25. A. J. Bard and L. R. Faulkner, *Electrochemical Methods* (John Wiley & Sons, New York) p. 305 (2001).
26. T. Shinagawa, A. T. Garcia-Esparza, and K. Takanabe, *Sci. Rep.*, **5**, 13801 (2015).
27. L. Stolz, G. Homann, M. Winter, and J. Kasnatscheew, *Mater. Today*, **44**, 9 (2021).

28. D. A. Noren and M. A. Hoffman, *J. Power Sources*, **152**, 175 (2005).
29. K. Park, B.-Y. Chang, and S. Hwang, *ACS Omega*, **4**, 19307 (2019).
30. H. J. S. Sand, *Philosophical Magazine Series*, **6**, 45 (1901).
31. H. Yan, K. Tantratian, K. Ellwood, E. T. Harrison, M. Nichols, Y. Cui, and L. Chen, *Adv. Energy Mater.*, **12**, 2102283 (2022).
32. Y. Liu et al., *Adv. Sci.*, **8**, 2003301 (2021).
33. X. L. Zhang, Z. H. Jiang, Z. P. Yao, Y. Song, and Z. D. Wu, *Corros. Sci.*, **51**, 581 (2009).
34. S. Anantharaj, S. Noda, M. Driess, and P. W. Menezes, *ACS Energy Lett.*, **6**, 1607 (2021).
35. S. Anantharaj and S. Noda, *J. Mater. Chem. A*, **10**, 93 (2022).
36. S. Anantharaj and S. Noda, *Materials Today Energy*, **29**, 101123 (2022).
37. S. Randau et al., *Nat. Energy*, **5**, 259 (2020).
38. M. Batzer, K. Voges, W. Wang, P. Michalowski, and A. Kwade, *Materials Today Communications*, **30**, 103189 (2022).
39. M. Keller, A. Varzi, and S. Passerini, *J. Power Sources*, **392**, 206 (2018).
40. J.-M. Doux, H. Nguyen, D. H. S. Tan, A. Banerjee, X. Wang, E. A. Wu, C. Jo, H. Yang, and Y. S. Meng, *Adv. Energy Mater.*, **10**, 1903253 (2019).
41. S.-K. Otto, T. Fuchs, Y. Moryson, C. Lerch, B. Mogwitz, J. Sann, J. Janek, A. Henss, and A. C. S. Appl, *Energy Mater.*, **4**, 12798 (2021).
42. J. Sakamoto, *Nat. Energy*, **4**, 827 (2019).
43. J. Kasemchainan, S. Zekoll, D. S. Jolly, Z. Ning, G. O. Hartley, J. Marrow, and P. G. Bruce, *Nat. Mater.*, **18**, 1105 (2019).
44. J.-S. Kim et al., *Nat. Commun.*, **14**, 782 (2023).